# Supramolecular Structures of the Chlorophyll *a*′ Aggregate and the Origin of the Diastereoselective Separation of Chlorophyll *a* and *a*′

**Toru Oba,[†] Hiroyasu Furukawa,[‡] Zheng-Yu Wang,[§] Tsunenori Nozawa,[§] Mamoru Mimuro,[||] Hitoshi Tamiaki,[†] and Tadashi Watanabe*[,‡]**

*Department of Bioscience and Biotechnology, Ritsumeikan University, Kusatsu, Shiga 525-8577, Japan*

*Received: January 30, 1998; In Final Form: May 19, 1998*

The supramolecular structure of the aggregate of chlorophyll *a*′ (Chl *a*′, the C13[2]-(*S*)-epimer of Chl *a*) was examined in comparison with that of the Chl *a* aggregate. The Chl *a*/*a*′ aggregate colloids were formed in aqueous alcohols, and IR, resonance Raman, and small-angle X-ray scattering (SAXS) measurements were performed on lyophilized precipitates of the aggregate colloids. The analyses on the Chl *a* colloidal precipitate obtained from a 26/74 2-propanol/$H_2O$ solution demonstrated that the supramolecular structure was similar to those of the aggregates of hydrated Chl *a*. On the other hand, the vibrational spectra of the Chl *a*′ colloidal precipitate formed in 40/60 MeOH/$H_2O$ were quite similar to those of anhydrous Chl *a* aggregates. A trace hydroxyl stretching IR absorption (at around 3350 $cm^{-1}$) of the Chl *a*′ aggregate precipitate was as small as that which the anhydrous Chl *a* aggregates could show. A SAXS profile of the Chl *a*′ colloidal precipitate demonstrated a lamellar structure with a 52-Å bilayer spacing, 8 Å greater than that of the Chl *a* aggregate formed in the 2-propanol/water. It was supposed that the Chl *a*′ aggregate was essentially anhydrous even in aqueous alcohols, while the Chl *a* aggregate was hydrated or swollen. A possible model of the supramolecular structure of the Chl *a*′ aggregate precipitate is presented. It is concluded that the difference between the supramolecular structures of the Chl *a* and *a*′ aggregates does not depend simply on the steric hindrance between the bulky substituents at the C13[2] and C17 positions but also on the possibility to form rigid intermolecular hydrogen-bonding networks. This is the origin of the diastereoselective separation of Chl *a* and *a*′, and it is also closely correlated to a structural degradation of the Chl *a*′ aggregate that occurs during the preparation of the colloidal precipitate.

## Introduction

To date, increasing attention has been paid to supramolecules which function as "energy transfer wires".[1−4] In addition to synthetic molecular arrays composed of a few molecules, more highly associated pigment systems such as self-assemblies of chlorophylls (Chl's) have been of interest to mimic and elucidate the structure and function of the naturally occurring energy transfer wire, chlorosome, in green photosynthetic bacteria.[5−9] There have so far been only a few works that deal with the supramolecular structures of such Chl aggregates in a colloidal dimension,[10−12] except for analyses on the crystals of Chl *a* derivatives with "short" C17-propionic ester chains (methyl- and ethyl-chlorophyllide *a* dihydrate and methyl-pyrochlorophyllide *a* monohydrate, Figure 1).[13−16] Worcester et al. employed the small angle neutron scattering (SANS) technique to elucidate the colloidal structure of the 740-nm-absorbing Chl *a* aggregate formed in a wet hydrocarbon such as octane and found that the aggregate was a cylindrical micelle 5.7 nm in diameter and hundreds of nanometers long.[10] Kratky et al. applied small-angle X-ray scattering (SAXS) measurements on a powder of microcrystalline Chl *a* and determined its supramolecular structure to be a lamella with an interlayer spacing of 42 Å.[11] The surface of the cylinder and the layers of the lamella were both supposed to be a two-dimensional sheet composed of hydrated Chl *a* molecules whose macrocycles were partially stacked and cross-linked by intermolecular hydrogen-bonding/coordination networks between the carbonyl moieties and the Mg atom. Worcester et al. also examined the effect of variation of the macrocycle (BChl *a*), the presence of a hydroxyl group

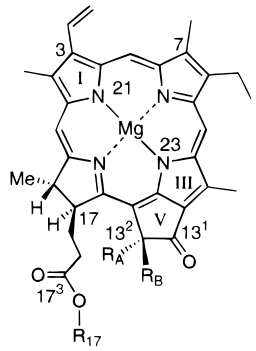


**Figure 1.** Molecular structure of Chl *a*, Chl *a*′, and their derivatives with partial numbering according to the IUPAC system: Chl *a*, $R_A$ = $COOCH_3$, $R_B$ = H, $R_{17}$ = phytyl; Chl *a*′, $R_A$ = H, $R_B$ = $COOCH_3$, $R_{17}$ = phytyl; methyl-chlorophyllide *a*, $R_A$ = $COOCH_3$, $R_B$ = H, $R_{17}$ = methyl; ethyl-chlorophyllide *a*, $R_A$ = $COOCH_3$, $R_B$ = H, $R_{17}$ = ethyl; methyl-pyrochlorophyllide *a*, $R_A$ = $R_B$ = H, $R_{17}$ = methyl.

* To whom correspondence should be addressed: phone and fax: +81-3-3401-5975; e-mail: watanabe@cc.iis.u-tokyo.ac.jp.

[†] Ritsumeikan University.

[‡] Institute of Industrial Science, University of Tokyo, Roppongi, Minato-ku, Tokyo 106, Japan.

[§] Department of Biochemistry and Engineering, Faculty of Engineering, Tohoku University, Sendai 980-77, Japan.

[||] National Institute for Basic Biology, Myodaiji, Okazaki 444, Japan. Present address: Department of Physics, Biology and Informatics, Faculty of Science, Yamaguchi University, Yoshida, Yamaguchi 753, Japan.

S1089-5647(98)00956-0 CCC: $15.00 
Published on Web 09/12/1998

at the C3[1] position (BChl *c*), and the absence of a central metal atom (Pheo *a*) on the cylindrical structures.[10] However, no comparable study has been performed yet on the effect of chirality of Chl to the supramolecular structure.

Chl *a*′ is the C13[2]-(*S*)-epimer of Chl *a*. The C13[2]-methoxycarbonyl moiety and C17-long aliphatic chain of Chl *a*′ both protrude to the same side of the macrocycle (Figure 1). Chl *a*′ is thermodynamically less stable than Chl *a* due to the steric hindrance between these bulky substituents (the equilibrium Chl *a*′ mole fraction = 0.24, see ref 17). Though visible absorption[18,19] and fluorescence spectra (Oba et al., unpublished results) and redox properties (Mazaki et al. and Iijima et al., unpublished results) of Chl *a* and *a*′ are almost the same due to a common $\pi$-conjugated system, the epimers are distinguished from each other by NMR[20,21] and CD spectra,[18,19] rate of pheophytinization (demetalation),[22−24] reducibility of the C13[1]-keto carbonyl moiety,[24] and elution behaviors in high-performance liquid chromatography (HPLC).[25] Hynninen and co-workers reported that Chl *a*′ was more soluble[23] and had a somewhat weaker intermolecular aggregation tendency in nonpolar organic solvents than Chl *a*.[23,26] They also reported an intriguing finding of the stereoselective separation of Chl *a* and *a*′:[26,27] Chl *a* dissolved in light petroleum readily formed a precipitate upon the solution being washed with water, while Chl *a*′ did not precipitate unless the solution was concentrated and then stored at −20 to −30 °C for 1−3 days. The visible absorption spectrum of Chl *a*′ in the wet light petroleum showed only a small shoulder at around 680−690 nm,[26] which was reminiscent of those of Chl *a* oligomers in nonpolar organic solvents.[28,29] The precipitated Chl *a*′ redissolved in benzene-$d_6$ showed an $^1$H NMR spectrum similar to that of the Chl *a* aggregate formed in nonpolar media.[23,26] Though it was reported that Chl *a*′ did not form precipitous Chl−water adducts as did Chl *a* due to the steric hindrance,[23,26,27] the supramolecular structure of the Chl *a*′ aggregate has not been examined yet, possibly because the absorption spectra of the Chl *a* and *a*′ aggregates in nonpolar solvents were similar to each other[26,30] and Chl *a*′ had long been regarded as merely an artifact produced in the course of handling of plant extracts. The origin of the diastereoselective phenomenon is still a subject to be tackled.

Recently, we studied aggregation of Chl *a*′ in aqueous media[31−33] in relation to a possible function of Chl *a*′ found in photosynthetic reaction center complexes of oxygen-evolving organisms.[34,35] The Chl *a*′ aggregate formed in aqueous methanol showed unique photophysical and colloidal properties: a formation of an almost single aggregate species whose $Q_y$ absorption band showed a small red-shift and explicit exciton splitting ($\lambda_{max}$, 690 and 715 nm), in contrast to a broad 750-nm absorption band of the Chl *a* aggregate in the same medium. Such a characteristic property of this Chl *a*′ aggregate, a novel energy transfer wire, prompted us to examine its supramolecular structure. This work was aimed at elucidating the colloidal structure of the Chl *a*′ aggregate formed in aqueous methanol. SAXS measurements and IR and resonance Raman (RR) spectroscopies were performed on the lyophilized colloidal precipitate. The results were compared with those of the stable Chl *a* aggregate colloid formed in aqueous 2-propanol. The model supramolecular structure of the Chl *a*′ aggregate colloid is proposed on the basis of these analyses, and the differences between the supramolecular structures of the Chl *a* and *a*′ aggregates reveal the origin of the stereoselective separation or the mechanism by which the chirality of Chl influences the aggregate structure.

## Materials and Methods

**Materials.** The preparation of pure Chl *a* and *a*′ has been described previously.[19,25,32,33] Briefly, Chl *a* was extracted from lyophilized spinach leaf tissues and was purified using preparative normal-phase HPLC (column, Senshupak Silica-5251N, 20 mm diameter × 250 mm, 4 °C; eluent, 100/0.8/0.4 hexane/2-propanol/methanol). Chl *a*′ was obtained by partial epimerization of Chl *a* followed by the same purification by HPLC. Prescribed amounts of Chl's (about 100 nmol, pigment purity >99%) were stored in 5-mL glass vials in solid form at −30 °C until use. The integrity of the pigment was ensured by analytical silica HPLC (column, Senshupak Silica-1251N 4.6 mm diameter × 250 mm, 4 °C; eluent, 100/0.8/0.4 hexane/2-propanol/methanol), visible absorption and circular dichroism (CD) spectra, elemental analysis, $^1$H NMR, and FAB-MS.[19,25]

HPLC-grade hexane, methanol, and 2-propanol were purchased from Wako Pure Chemicals, Ltd., and were used without further purification. Water purified with a Milli-Q system (Millipore Ltd.) was used throughout.

**Preparation of Chl *a* and *a*′ Aggregate Colloids.** The Chl aggregate particles were obtained by centrifugation of colloidal solutions. A methanol solution of Chl *a*′ (100 nmol/2 mL) was diluted quickly with water (3 mL) in the glass vial, followed by stirring for 3 min.[32,33] The mixed solutions (nearly 20 $\mu$M, on the monomer basis) were incubated for about 24 h at 25 °C under dark. The formation of the aggregate was examined by visible absorption spectroscopy ($\lambda_{max}$ = 690 and 715 nm). The Chl *a*′ aggregate colloidal solutions were centrifuged (30000−40000 rpm, 30 min, 25 °C), and the precipitates were lyophilized. The Chl *a* aggregate colloid was formed in 26/74 2-propanol/$H_2O$ ($\lambda_{max}$ = 746 nm; incubation, 3 days), and colloidal precipitates were prepared in the same manner as above. The solid samples were further pumped at room temperature before the measurements.

**Instrumentation.** Visible absorption spectra of the aggregate solutions were recorded on a Hitachi spectrophotometer, model 330. IR spectra of the colloidal precipitates were obtained using a technique of reflection absorption spectroscopy. The measurements were performed on solid films prepared by deposition of the lyophilized precipitates on an aluminum plate. A Shimadzu FTIR-8600 spectrometer equipped with an AIM-8000R IR microscope was employed with a resolution of 4 cm$^{-1}$. RR spectra of the Chl *a* and *a*′ aggregates (solutions and precipitates) were obtained with 4 cm$^{-1}$ resolution using a Jobin-Yvon Raman system T 64000. The sample solid was put into a hole (1 mm diameter × 2 mm) of a metal plate and was irradiated with the 457.9-nm line of an $Ar^+$ laser (NEC GLG-3460, ∼20 mW).

SAXS measurements were carried out at the BL10C station in the Photon Factory (National Laboratory for High Energy Physics, Tsukuba, Japan). A monochromic X-ray with a wavelength ($\lambda$) of 1.448 Å irradiated the sample (roughly 5 mg, packed in a glass capillary) placed just in front of a position-sensitive proportional counter (PSPC). The scattering data were accumulated over a period of 2 h and then corrected for the scattering from the empty cell.

## Results

**Chl *a* and *a*′ Aggregate Colloids Dispersed in Solutions.** First, we briefly describe several spectroscopic characteristics of the Chl *a* and *a*′ aggregates formed and dispersed in aqueous alcohols. Figure 2 illustrates visible absorption and RR spectra of the Chl *a* and *a*′ aggregates. The broken curve in Figure 2a is the visible absorption spectrum of the Chl *a* aggregate formed

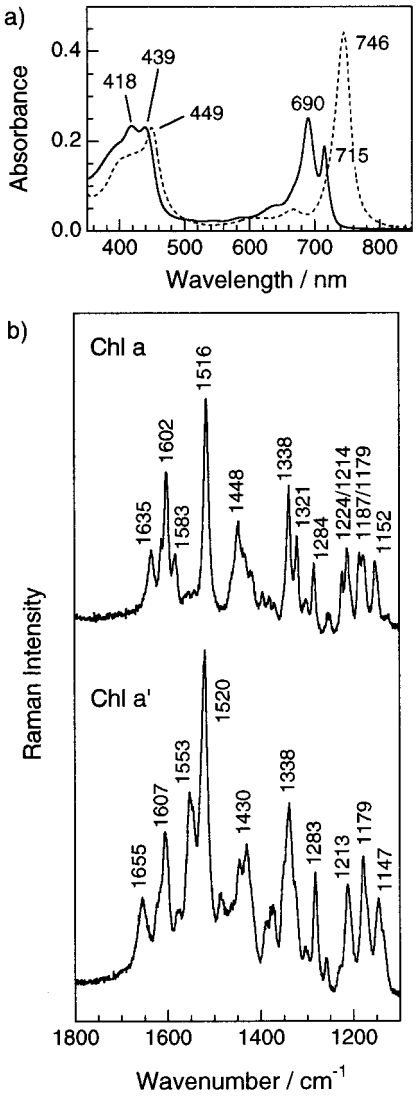


**Figure 2.** Visible absorption and resonance Raman spectra of the stationary Chl *a* and *a*′ aggregates in aqueous alcohols: (a) visible absorption spectra (5 $\mu$M, on monomer basis, 25 °C), solid curve, Chl *a*′ aggregate formed in 40/60 MeOH/$H_2O$; broken curve, Chl *a* aggregate formed in 26/74 2-PrOH/$H_2O$ and (b) resonance Raman spectra, upper curve, Chl *a* aggregate (50 $\mu$M, on monomer basis); lower curve, Chl *a*′ aggregate (100 $\mu$M, on monomer basis).

in 26/74 2-propanol/water (5 $\mu$M, on the monomer basis), the conditions where the typical, more stable 750-nm-absorbing form was obtained with better reproducibility than in aqueous methanol.[33] The aggregate formed in the aqueous 2-propanol gives an intense $Q_y$ absorption band at 746 nm and the Soret peak at 449 nm. The 746-nm band has a width (full width at half-maximum) of 520 $cm^{-1}$, as sharp as that of monomeric Chl *a* in methanol.[32,33] The amplitude of this red-shifted $Q_y$ band is roughly 2-fold larger than that of the Soret maximum. The absorption spectral feature is similar to those of previously reported hydrated Chl *a* aggregates in wet nonpolar solvents and in solid states.[11,36−42] The CD spectrum of the aggregate in the aqueous 2-propanol showed a considerably deep trough at 740−750 nm (around −1000 mdeg for the 5 $\mu$M sample) and much smaller components in the Soret region (ca. ±130 mdeg). This aggregate also gave a fluorescence emission band at 750−753 nm. The size of the Chl *a* aggregate colloid was so large (>1 $\mu$m) that dynamic light scattering (DLS) measurement of the aggregate solution (5 $\mu$M, on the monomer basis; in 2-propanol/water) was hampered by critical opalescence.

The upper curve in Figure 2b depicts the RR spectrum of this Chl *a* aggregate (50 $\mu$M, on the monomer basis). Raman lines in the wavenumber region over 1100−1400 $cm^{-1}$ originate mainly from the C−H and C−N bonds in the chlorin macrocycle and the peripheral substituents, and vibrational bands at 1516, 1583, and 1602 $cm^{-1}$ originate from C═C stretching of the macrocycle skeleton.[44] No scattering band is noted at around 1550 $cm^{-1}$, and three RR peaks appear in the range of 1580−1620 $cm^{-1}$; such a spectral feature resembles those of hydrated Chl *a* aggregates.[43] A band at 1635 $cm^{-1}$ is assigned to the $C13^1$-keto carbonyl stretching vibration. The wavenumber position of this keto band matches those of the IR/RR bands of hydrated Chl *a* aggregates[39,41−43] and is heavily downshifted (∼35 $cm^{-1}$) from that of monomeric Chl *a* (∼1670 $cm^{-1}$ in methanol, refs 43, 45, and 46); this suggests that the moiety was involved in tight hydrogen bonding.

On the other hand, Chl *a*′ yielded a unique aggregate species in 40/60 methanol/water. The solid curve in Figure 2a is the visible absorption spectrum of the Chl *a*′ aggregate (5 $\mu$M, on the monomer basis). The sharp, double-peaked absorption bands are observed at 690 and 715 nm. The Soret absorption peaks are at 439 and 418 nm. The amplitudes of the $Q_y$ and Soret absorption peaks are roughly comparable to each other. There is no absorption band in the wavelength region longer than the 715-nm peak. This aggregate species gave the dispersed-type CD signals at 694 nm (+) and 715 nm (−) and the fluorescence peak at 718−719 nm.[32,33] Fluorescence polarization measurements demonstrated that both the 690- and the 715-nm bands of the double-peaked absorption originated in a common single-aggregate species.[32] The colloidal size of the Chl *a*′ aggregate was found to be ca. 130 nm in diameter by the DLS measurements.[33]

The RR spectrum of the Chl *a*′ aggregate (100 $\mu$M, on the monomer basis; lower curve in Figure 2b) is different from that of the Chl *a* aggregate. The central Mg atom of Chl *a*′ in the aggregate was in the five-coordinated state as judged from the locations of the coordination-sensitive C═C Raman lines at 1520, 1553, and 1607 $cm^{-1}$.[45] The $C13^1$-keto carbonyl band was observed at 1655 $cm^{-1}$, downshifted from that of the Chl *a* monomer (∼1670 $cm^{-1}$ in methanol)[43,45,46] to a lesser extent than in the Chl *a* aggregate (1635 $cm^{-1}$, upper curve in Figure 2b). The wavenumber position of this keto band, as well as the finding that this keto RR line stayed still even when the Chl *a*′ aggregate was prepared in a fully deuterated solvent (40/60 $CD_3OD/D_2O$), suggested that in the aggregate the $C13^1$-keto carbonyl moiety of one Chl *a*′ molecule preferred a direct coordination interaction with the Mg atom of another Chl *a*′ molecule to that with a solvent molecule.[32]

For SAXS measurements with better resolution and for IR spectroscopy in the hydroxyl stretching region, the analyses should be performed on dry solid samples. Colloidal precipitates of the Chl *a* and *a*′ aggregates were collected from the solutions of high concentration (20 $\mu$M, on the monomer basis) which gave essentially the same absorption spectra as that shown in Figure 2. Centrifugation of the 20 $\mu$M aggregate solutions yielded green, minute particles and a stiff paste. Vibrational spectra and SAXS profiles were obtained for such precipitates after lyophilization.

**IR Spectra of the Chl *a* and *a*′ Aggregate Precipitates.** Figures 3 and 4 depict the IR spectra of the precipitates of the Chl *a* and *a*′ aggregate colloids formed in 26/74 2-PrOH/$H_2O$ and 40/60 MeOH/$H_2O$, respectively. The IR spectrum of the Chl *a* precipitate resembles those of the previously reported hydrated Chl *a* polymers both in C═O/C═C and O−H/C−H

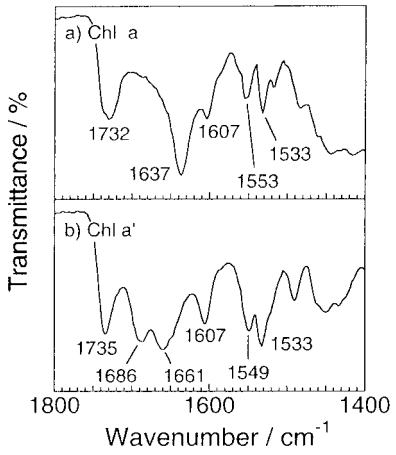


**Figure 3.** IR spectra (carbonyl and C═C stretching region) of Chl *a* (a) and Chl *a*′ (b) colloidal precipitates.

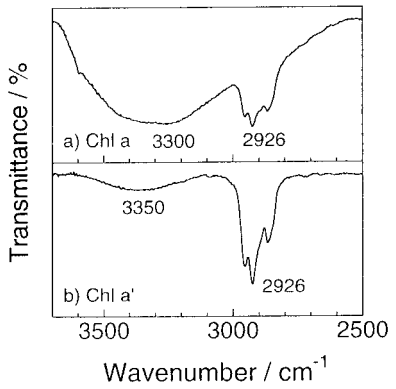


**Figure 4.** IR spectra (hydroxyl stretching region) of Chl *a* (a) and Chl *a*′ (b) colloidal precipitates.

stretching regions (Figures 3a and 4a).[36,39,41,42] The Chl *a* colloid obtained from aqueous 2-propanol shows a broad IR absorption band at 1732 $cm^{-1}$ arising from the $C13^2$- and $C17^3$-ester carbonyl stretching vibrations (Figure 3a). A strong IR band at 1637 $cm^{-1}$ is assigned to the $C13^1$-keto carbonyl moiety tightly hydrogen bonded to a water (or a methanol) molecule.[39,41,42] This keto vibrational band stayed at nearly the same wavenumber position throughout the processes of the centrifugation and lyophilization (Figures 2b and 3a). The IR bands at 1607, 1533, and 1553 $cm^{-1}$ arise from the C═C skeletal vibrations of the chlorin macrocycle. The five-coordinated state of the Mg atom of Chl *a* molecules in the aggregate was deduced from the wavenumber positions of the former two C═C bands.[45]

Figure 4a shows the 2500−3700 $cm^{-1}$ region of the IR spectrum of the Chl *a* aggregate colloidal precipitate. Sharp IR absorption bands at 2868, 2926, and 2953 $cm^{-1}$ are attributed to the vibrations of C−H bonds in the chlorin macrocycle and the peripheral substituents. A hydroxyl absorption band peaking at around 3300 $cm^{-1}$ is quite wide and strong, indicating an involvement of solvent molecules in the precipitate. This is consistent with an observation of the broad absorptions at around 1400 $cm^{-1}$ (O−H bending; Figure 3a) and around 1050 $cm^{-1}$ (C−O stretching; data not shown). The broad 3300-$cm^{-1}$ band comprises several spectral components of different molar absorptivities originating from OH groups under different hydrogen-bonding conditions. Such an enormous OH band is similar to that given by the Chl *a* aggregate prepared in wet $CCl_4$ at 3−8 °C[47] but is larger than that observed for a film of a polymer of monohydrated Chl *a*, $(\text{Chl } a \cdot H_2O)_n$.[42]

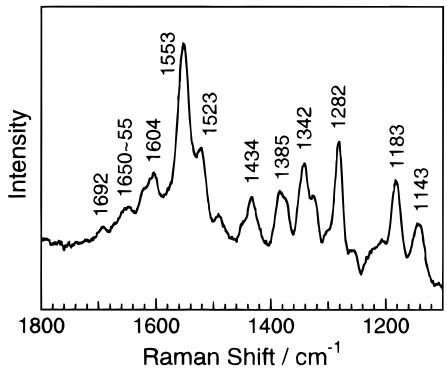


**Figure 5.** Resonance Raman spectrum of Chl *a*′ colloidal precipitate.

Vibrational spectra of the Chl *a*′ aggregate precipitate collected from the aqueous methanol (Figures 3b and 4b) were totally different from those of the Chl *a* aggregate mentioned above (Figures 3a and 4a) and were quite similar to those of anhydrous Chl *a* dimers or oligomers formed in dry carbon tetrachloride or dry *n*-butylcyclohexane or in a solid state.[41,42,48,49] The Chl *a*′ aggregate colloid formed in 40/60 $MeOH/H_2O$ gives an ester absorption band at 1735 $cm^{-1}$, sharper than that of the above Chl *a* aggregate (1732 $cm^{-1}$, Figure 3a). The IR bands at 1607 and 1533 $cm^{-1}$ originating from the macrocycle C═C vibrations demonstrate the five-coordinated state of the Mg atom in the aggregate.[45] It is noted that the Chl *a*′ colloid gives two $C13^2$-keto IR bands of roughly equal intensities at 1661 and 1686 $cm^{-1}$, indicating that the $C13^1$-keto carbonyl moieties exist under two different circumstances in the common Chl *a*′ colloidal precipitate. This is in sharp contrast to the detection of only one keto RR band at 1655 $cm^{-1}$ before the preparation of the precipitate (Figure 2b). The discrepancy indicates that the Chl *a*′ aggregate structure was damaged during the processes of centrifugation and lyophilization. The former 1661-$cm^{-1}$ absorption matches the RR scattering band in Figure 2b (1655 $cm^{-1}$) and is assigned to the $C13^1$-keto group coordinating to the Mg atom of a neighboring Chl molecule.[32,33] The 1686-$cm^{-1}$ band, absent in Figure 2b, comes from the $C13^1$-keto group free from any coordination and hydrogen bonding,[41,42,49] as judged from the higher wavenumber position than the RR band of the keto group hydrogen bonded to methanol (∼1670 $cm^{-1}$).[43,45,46]

In the C−H stretching region (2850−3000 $cm^{-1}$, Figure 4b), the Chl *a*′ aggregate gave IR bands almost common to those of the Chl *a* aggregate (Figure 4a). A considerable difference between the Chl *a* and *a*′ aggregate spectra exists in the amplitudes of hydroxyl absorption bands (3000−3700 $cm^{-1}$). The Chl *a*′ colloid shows a quite small absorption at the same wavenumber region where the Chl *a* aggregate gave the enormous one (Figure 4a). The slight 3350-$cm^{-1}$ OH band of the Chl *a*′ precipitate arises from the hydrogen-bonded water (or methanol) molecules, while a carbonyl overtone could also appear in the same region.[41,42] The area of this OH absorption band was roughly equal to that of a 3320-$cm^{-1}$ absorption given by a film of a Chl *a* dimer monohydrate, $(\text{Chl } a)_2 \cdot H_2O$ (ref 42; areas were normalized by the intensities of the 2924−2926 $cm^{-1}$ bands).

**RR Spectra of the Chl *a*′ Aggregate Precipitate.** Figure 5 illustrates the RR spectrum of the precipitate of the Chl *a*′ aggregate measured by excitation at 457.9 nm. There are several differences between the RR spectra obtained before (Figure 2b) and after (Figure 5) the centrifugation and lyophilization of the colloid. The most remarkable one is an observation of two $C13^1$-keto carbonyl bands at around 1650−1655 and 1692 $cm^{-1}$

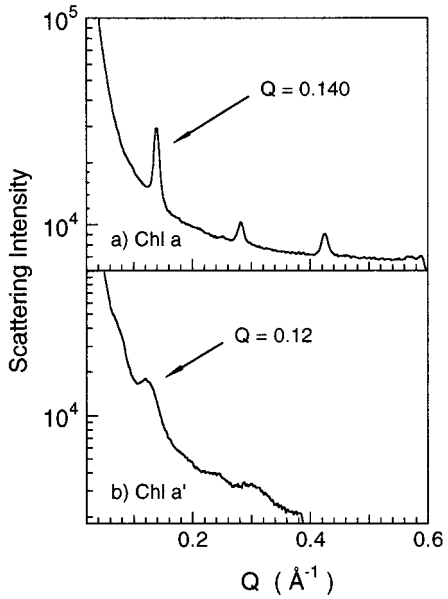


**Figure 6.** Small-angle X-ray scattering profiles of the Chl *a* (a) and Chl *a*′ (b) colloidal precipitates as a function of $Q = 4\pi \sin \theta/\lambda$ (Å$^{-1}$).

in Figure 5. These RR scattering bands correspond well to the two keto IR bands observed in Figure 3b (at 1661 and 1686 cm$^{-1}$). It can be said that the C13$^1$-keto carbonyl moiety coordinating to the Mg atom was responsible for both the RR band at 1650−1655 cm$^{-1}$ and the IR band at 1661 cm$^{-1}$ and the 1692-cm$^{-1}$ RR line and the 1686-cm$^{-1}$ IR band are assignable to the free keto band. It is strongly suggested that both the ∼1655- and the ∼1690-cm$^{-1}$ vibrational bands arise from the component molecules of the aggregate but not from the monomeric Chl *a*′, which could coexist in the damaged aggregate sample. The monomer did not give substantial RR scattering bands when the sample was irradiated at 458 nm, since the monomer does not have sufficient absorption at 458 nm and excitation energy should not migrate uphill from the aggregate to the monomer.

Other differences between Figures 2b and 5 are found in the relative intensities of the Raman lines. The ∼1555-cm$^{-1}$ band is more intense than the ∼1525-cm$^{-1}$ band in Figure 5, in contrast to that in Figure 2b.[32,33] The relative intensities of the ∼1555- and ∼1525-cm$^{-1}$ bands reversed during the preparation of the precipitate. The absence of the band at around 1215 cm$^{-1}$ and the presence of the relatively intense ∼1285-cm$^{-1}$ band are also characteristics of the precipitate (Figure 5). The intensity pattern in Figure 5 resembles those of monomeric Chl *a* in various media[43,45,46] and those of Chl *a* and *a*′ aggregates of "T-shaped" conformation.[32,33,43] Such a spectral transformation reflects the degradation of the aggregate structure.

The coordination-sensitive C═C bands were observed at 1523, 1553, and 1604 cm$^{-1}$ in Figure 5, showing little difference in the band positions from those in Figure 2b.[45] As demonstrated by the position of the 1553-cm$^{-1}$ band, the Mg atom in the precipitate was essentially in the five-coordinated state, which is consistent with what the IR spectrum suggested (Figure 3b).

**SAXS Profiles of the Chl *a* and *a*′ Aggregate Precipitates.** Figure 6a depicts the X-ray diffraction pattern of the precipitated Chl *a* aggregate formed in 26/74 2-propanol/water, as a function of scattering vector $Q = 4\pi \sin \theta/\lambda$, where $\theta$ is the half scattering angle and $\lambda$ is the wavelength. Three sharp diffraction peaks were clearly observed at $Q = 0.140$, 0.280, and 0.423 Å$^{-1}$, in addition to a small peak at $Q = 0.565$ Å$^{-1}$. Another SAXS measurement on the same sample over a wider scattering angle enabled an observation of the sixth diffraction peak at 0.853 Å$^{-1}$ (data not shown), indicating that the aggregate possesses a long-range ordered colloidal structure. This series of Bragg reflections with an interrelation of $1{:}{}^1/_2{:}{}^1/_3{:}{}^1/_4{:}({}^1/_5){:}{}^1/_6$ suggests that the Chl *a* aggregate colloid consists of a lamellar structure with an interplanar spacing of 44.5 Å. This result is similar to that of Kratky and Dunitz.[11]

On the other hand, the precipitate of the Chl *a*′ aggregate colloid formed in 40/60 MeOH/$H_2O$ (Figure 6b) gave a couple of much weaker peaks over the region of $Q = 0.05-0.4$ Å$^{-1}$. This indicates that some structural order still exists in the Chl *a*′ precipitate, though the degree of the order was much lower than that of the Chl *a* aggregate, as judged from the broadening of the diffraction peaks in Figure 6b compared to those in Figure 6a. The characteristic of the Chl *a*′ aggregate is the appearance of two peaks at $Q = 0.12$ and 0.24 Å$^{-1}$ with an interrelation of $1{:}{}^1/_2$. This suggests that the major component of the lyophilized Chl *a*′ aggregate colloidal particle may also possess a bilayer structure similar to that of Chl *a*, but with a larger interplanar distance of 52.2 Å, about 8 Å greater than that of the Chl *a* colloid. A broad diffraction at $Q = 0.3$ Å$^{-1}$ (corresponding to a 21-Å spacing) in Figure 6b may arise from some minor structures coexisting in the precipitate.

## Discussion

**Supramolecular Structure of the Chl *a* Aggregate Precipitate.** There have been many reports on the 740−760-nm-absorbing form of the Chl *a* aggregates in wet hydrocarbons or in films exposed to water vapor.[10,11,36−42,49] Chlorophyllide *a* esterified with primary alcohols also gave similar aggregate spectra.[11,38] These aggregates were interpreted as ordered molecular arrays of hydrated Chl *a* in which the Chl molecules cross-linked together with water molecules by hydrogen bondings and coordination interactions.[10,11] Such a species commonly exhibited a largely downshifted C13$^1$-keto carbonyl stretching band (at around 1640 cm$^{-1}$) due to tight hydrogen bonding to a water molecule.[36,39,41,42] The ester IR band was broadened or split, also reflecting the hydration, and there was a broad hydroxyl absorption of the solvents in the higher wavenumber region.[36,41,42,47] Kratky and Dunitz interpreted a detailed X-ray diffraction pattern of such a 740-nm-absorbing microcrystalline Chl *a* as double layers of hydrated Chl molecules with a lamellar spacing of 42 Å. These structural characteristics were also preserved in our Chl *a* aggregate. It is concluded that the Chl *a* aggregate colloid formed in aqueous 2-propanol possessed a lamellar structure (layer spacing, 44.5 Å) composed of a molecular array of cross-linked hydrated Chl *a*. Though Worcester et al. reported the formation of the cylindrical micelle,[10] it is plausible that the layer of the hydrated Chl *a* lamella corresponds to the fragment of the cylindrical micelle and could grow into the cylinder under appropriate conditions.

This work cannot derive the exact hydration number of Chl *a* in the aggregate. The degree of hydration of Chl *a* in the aggregated forms has been a matter of dispute.[49,50,51] The cylindrical micelle formed in wet hydrocarbon was modeled as an associate of dihydrated Chl *a*,[10] while the lamellar structure of the microcrystalline form was thought to be composed of monohydrated Chl *a*.[11] It was also reported that various hydration numbers were possible when the Chl *a* aggregate film was prepared in the presence of a separate water phase.[49] We assume that the Chl *a* aggregate formed in aqueous 2-propanol was swollen: a difference in spacing of 2.5 Å compared with

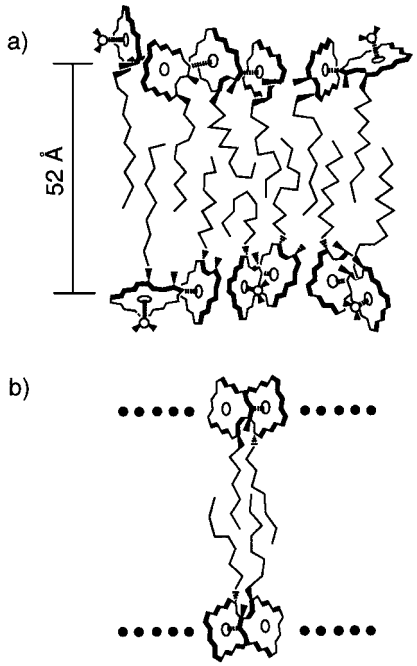


**Figure 7.** Schematic representation of the model supramolecular structures of Chl *a*′ aggregate colloid: (a) damaged aggregate structure after centrifugation and lyophilization and (b) a model of the original aggregate structure before structural degradation.

the result of Kratky and Dunitz may reflect a structural part of an "excess" water network which resisted lyophilization and pumping. It is noteworthy that the Chl *a*′ aggregate precipitate involved a considerably smaller amount of water (or alcohol) than this Chl *a* colloidal precipitate despite the same drying processes. This is crucial for the estimation of the supramolecular structure of the Chl *a*′ aggregate as well as an origin of the transformation during the preparation of the precipitate.

**Model Supramolecular Structure of the Chl *a*′ Aggregate Precipitate.** Chl *a* forms anhydrous dimers or oligomers in dry carbon tetrachloride, dry *n*-butylcyclohexane, and dry *n*-hexane and in the solid state.[41,42,48,49] The IR spectra of these aggregates showed clear contrasts to those of the hydrated aggregates. An ester carbonyl IR band (at 1735−1740 $cm^{-1}$) was sharp, suggesting that neither the $C13^2$- nor the $C17^3$-carbonyl group was hydrated. The two IR bands observed at 1650−1660 and 1690−1700 $cm^{-1}$ were assigned to the coordinated and uncoordinated $C13^1$-keto carbonyl groups. The five-coordination of the Mg atom can be deduced from observations of a skeletal vibration at 1608−1610 $cm^{-1}$. The anhydrous Chl *a* aggregates could involve a trace of water which gave a small absorption at around 3350 $cm^{-1}$. These are also the characteristics of the present Chl *a*′ aggregate colloidal precipitate: the sharp ester carbonyl band at 1735 $cm^{-1}$, the coordinated and uncoordinated keto bands at ∼1655 and ∼1690 $cm^{-1}$, the five-coordinated Mg atoms, and the involvement of water (or methanol) molecules whose amount was as small as that in the Chl *a* anhydrous aggregate species. On the basis of such close similarities in the vibrational spectra, it is reasonable to assume that Chl *a*′ molecules in the aggregate precipitate are associated with a conformation similar to those in the anhydrous dimers (oligomers) of Chl *a*.[28,41,52,53]

Figure 7a illustrates a model supramolecular structure of the major part of the Chl *a*′ aggregate precipitate. The precipitate possesses a lamellar structure with an interplanar distance of 52.2 Å. The chlorin macrocycles associate to form layers, and the phytyl chains make up a somewhat disordered region between the macrocycle layers. The $C13^1$-keto carbonyl moiety of one Chl *a*′ molecule directly coordinates to the Mg atom of a neighboring molecule, and these macrocycles form a T-shaped conformation as in the anhydrous Chl *a* aggregates.[28,41,52,53] This T-shaped dimer can further interact with other molecules in the same manner, resulting in the formation of T-shaped oligomers. The $C13^1$-keto carbonyl group of the one terminal Chl of the T-shaped oligomer is free from any coordination and hydrogen bonding, and the Mg atom of the other terminal Chl is hydrated (or solvated).

The T-shaped conformation of the Chl *a*′ oligomer is supported by the intensity pattern of the Raman lines in the C═C and C−N stretching region.[43] The RR spectral features of the Chl *a*/*a*′ monomers and aggregates can be classified into roughly three patterns: type 1 (common for the monomer and the T-shaped aggregates in various media), in which a ∼1555-$cm^{-1}$ band is more intense than a ∼1525-$cm^{-1}$ band, a ∼1285-$cm^{-1}$ band is strong, and an intense band at around 1215 $cm^{-1}$ is absent or weak (Figure 5);[32,33,43,45,46,52] type 2 (characteristic of the aggregates formed in aqueous organic solvents), in which a ∼1555-$cm^{-1}$ band is less intense than a ∼1525-$cm^{-1}$ band, a ∼1285-$cm^{-1}$ band is relatively weak, and a strong band is present at around 1215 $cm^{-1}$ (lower curve in Figure 2b);[32,33,43,54] and type 3 (observed for the polymers of hydrated Chl *a*), for which a ∼1525-$cm^{-1}$ band is quite intense while a ∼1555-$cm^{-1}$ band is absent, three bands are located in 1580−1620 $cm^{-1}$ region, a ∼1285-$cm^{-1}$ band is weak, and a ∼1215-$cm^{-1}$ band is strong (upper curve in Figure 2b).[43] It was suggested that these RR intensity patterns reflect closeness of the stacked macrocycles in the aggregate structure, which could affect the macrocycle C═C and C−N vibrations.[43] In this context, the type 1 spectrum indicates the lack or looseness of the macrocycle stacking, and the molecular packing in the stacked structure is regarded to be tightened in going from type 2 to type 3. Thus, type 1 spectrum of the Chl *a*′ colloidal precipitate (Figure 5) suggests the T-shaped conformation, which is consistent with the above model deduced from the IR spectra.

It is difficult to determine the exact aggregation number of the T-shaped Chl *a*′ oligomer. It was reported that anhydrous Chl *a* aggregates gave coordinating and free keto IR bands whose wavenumber positions were nearly unchanged, with intensities that were not drastically different in the range of dimer to 16-mer.[48] On the other hand, another report revealed that the anhydrous Chl *a* polymers, $(Chl\ a)_n$, yielded substantially no free keto RR band.[43] It is plausible that the aggregation number of the T-shaped Chl *a*′ oligomer had some distribution, as judged from the somewhat broad 1661-$cm^{-1}$ IR band in Figure 3b. The observation of the coordinating (1655 $cm^{-1}$) and free (1690 $cm^{-1}$) keto carbonyl bands of comparable intensities (Figure 3b) suggests that the size of the T-shaped Chl *a*′ oligomer may peak at low aggregation numbers of, say, 2−20.

One may point out a drift of the RR spectrum of the Chl *a*′ aggregate precipitate toward being larger in the lower wavenumber region (Figure 5). The drift may be attributed to fluorescence (at around 500 nm) irradiated from an excited state corresponding to the Soret absorption. This implicates the existence of fluorescent Chl *a*′ species in the precipitate. In this context, there are three ways to rationalize the origins of the observed two keto vibrational bands (1655 and 1690 $cm^{-1}$, Figures 3b and 5). The first possibility is that both bands originated from the fluorescent aggregates; the T-shaped aggregates of small aggregation numbers could give fluorescence in the wavenumber region similar to that of the monomer. The

other two possibilities allow the coexistence of the monomer in the aggregate precipitate: in the second, both keto bands came from the "nonfluorescent (in the 500-nm region)" aggregates and the fluorescence from the monomer, and in the third, the 1655-$cm^{-1}$ band came from the aggregates while the 1690-$cm^{-1}$ one was from the monomer. For both of these cases, the RR intensity patterns of the spectral contributions from the aggregates can be regarded as those of the T-shaped aggregates. This leads to an illustration that monomeric Chl *a*′ molecules existed on the surface of the colloidal particle of the 'T-shaped' aggregate, because the electronic structure of the molecule buried into the molecular arrays in the aggregate should be perturbed. Thus, no essential change is required for the above model structure (Figure 7a).

**Model Supramolecular Structure of the Chl *a*′ Aggregate before Structural Degradation.** The supramolecular structure described above was the result of a transformation from an "original" structure that the aggregate possessed before the preparation of the precipitate. The structural degradation was demonstrated not only by the appearance of the free keto absorption band in the IR/RR spectrum (Figures 3b and 5) and the changes in the RR spectral feature (Figure 5) but also by the broadness of the SAXS diffraction peaks and the presence of the 0.3-$Å^{-1}$ SAXS peak arising from the minor coexisting structure (Figure 6b). As judged from the characteristic, sharp doublet absorption (Figure 2a), much higher order is expected in the original aggregate structure than in the above model. Prior to centrifugation and lyophilization, the single RR band at 1655 $cm^{-1}$ indicated the presence of a single type of the coordinating $C13^1$-keto carbonyl moiety in the Chl *a*′ aggregate (Figure 2c). The three-coordination-sensitive C═C bands demonstrated the five-coordination of the Mg atoms. The RR intensity pattern suggests the stacking of the Chl *a*′ macrocycles.[43] These structural constraints lead to two possible conformations of a J aggregate (each molecule links with two neighboring molecules) or a "closed" dimeric unit (two molecules fold together with the intermolecular interactions between mutual keto groups and Mg atoms, and such dimers behave as units to form the colloid). The observed double-peaked absorption spectrum (Figure 2a) supports the latter case rather than the former one.[32,55] It is reasonable to assume that the original Chl *a*′ aggregate also possessed a lamellar structure, because the Chl *a*′ colloidal precipitate still preserved the lamella structure even after the structural degradation.

Thus, we assume the supramolecular structure of the Chl *a*′ aggregate existing before the centrifugation and lyophilization processes to be as shown in Figure 7b: Chl *a*′ molecules form the closed dimers, and the dimers array to form layers in a lamellar structure. This may be reasonable in view of the fact that a "molecule" with two long alkyl chains tends to form a vesicle or a bilayer.[56] If a part of the molecular linkages (the intermolecular interactions between the keto groups and Mg atoms) in the dimers is removed, the "folded" dimer structure can open to be the T-shaped conformation (Figure 7a), resulting in the transformation of the supramolecular structure.

We also assume that Chl *a*′ molecules in the aggregate were associated without bridging water molecules before the preparation of the precipitate, as opposed to the structure of the hydrated Chl *a* aggregate.[57] The solvent molecules may permeate into the aggregate when the supramolecular structure is damaged, because the following findings did not suggest a special interaction between Chl *a*′ and water; (1) the $C13^1$-keto RR band of the Chl *a*′ aggregate was downshifted from that of the monomer to a lesser extent than the hydrogen-bonding keto band of the Chl *a* aggregate (Figure 2b), (2) the RR experiment employing the fully deuterated solvents suggested that the keto moiety preferred the C═O···Mg interaction to the solvation (C═O···$H_2O$ or MeOH),[32] (3) Chl *a*′ dissolved in light petroleum did not form precipitate upon the solution being washed with water, while Chl *a* readily precipitated as the water adducts,[27] (4) no Chl *a*′ dissolved in wet light petroleum precipitated unless the solution was concentrated and cooled to −20 °C (reducing the entropy of the aggregation),[27] and (5) the precipitated Chl *a*′ redissolved in benzene-$d_6$ showed an $^1H$ NMR spectrum similar to that of the anhydrous Chl *a* aggregates.[23,26] An illustration of a more detailed structure requires further investigation including theoretical approaches.

**Origin of the Different Aggregation Behaviors between Chl *a* and Chl *a*′.** The Chl *a* and *a*′ aggregates were distinguished from each other by the forces which held the supramolecular structures. Chl *a* tended to take up water molecules into the aggregate. Relatively strong, directional forces of hydrogen bondings between Chl and water molecules constituted the rigid molecular array which resisted the structural degradation during the preparation of the precipitate. Additional, weaker interactions of van der Waals forces and $\pi-\pi$ interaction[60] also contributed to the optimized structure. On the other hand, the aggregation of Chl *a*′ tended to keep the solvent molecules out of the pigment associate. Internal interactions in the Chl *a*′ aggregates were the coordination of $C13^1$═O···Mg, van der Waals forces, and $\pi-\pi$ interaction. The following three reasons suggest that the $C13^1$═O···Mg interaction may be weak and insufficient to maintain the supramolecular structure in comparison with the $C13^1$═O···$H_2O$···Mg interaction in the hydrated Chl *a* aggregate: (1) the $C13^1$═O···Mg coordination is roughly 60-fold weaker than the $C13^1$═O···MeOH (or $C13^1$═O···$H_2O$) interaction, as estimated from the equilibrium constant for Chl *a* dimer disaggregation,[61] (2) in the stacked structure, the coordination of $C13^1$═O···Mg could not be tightened without heavy bending of the pentagonal ring (ring V) due to the unfavorable location of the lone pair of electrons of the oxygen atom of the keto group, and (3) it was suggested that the steric hindrance between the C17- and $C13^2$-ester chains of Chl *a*′ pushed the latter moiety closer to the $C13^1$-keto carbonyl group and hindered the coordination of the $C13^1$-keto moiety.[23,51] The weak interactions of limited directionality could optimize the Chl conformation in the aggregate, while hydrophobic solvation, or the effect that surrounding solvent networks packed these Chl molecules into a small space, gave a large contribution to stabilizing the colloid. This may be a reason that the structural degradation occurred for the Chl *a*′ aggregate during the centrifugation and lyophilization processes.

The difference in the supramolecular structures of the 750-nm-absorbing Chl *a* aggregates and the Chl *a*′ aggregates does originate in the chirality at the $C13^2$-position but does not depend simply on the steric hindrance between the C17- and $C13^2$-ester chains. It should be said that the possibility for the formation of the rigid intramolecular hydrogen-bonding network distinguishes the structures, stability, and properties of these aggregate colloids, at least at around room temperature; this is the origin of the stereoselective separation of Chl *a* and *a*′. The chirality of the epimers is enhanced by their affinities to water. The difference in the affinities can be attributed to the properties of monomeric Chl *a*/*a*′. It is supposed that a (hydrated) Chl *a* monomer may have more hydrophilic surface than a (hydrated) Chl *a*′ monomer, because Chl *a*′ is more soluble in nonpolar solvents (i.e., it is harder to form the aggregate) than Chl *a*[23]

and Chl *a*′ is eluted earlier than Chl *a* from normal-phase HPLC and later from reversed-phase HPLC.[25] Such differences may further originate from the weaker electron-donating character of the C13[1]-keto carbonyl group of Chl *a*′ than that of Chl *a*[23,26] Another explanation might be possible as each diastereomer of hexoses has its own hydration number depending on the number of the equatorial hydroxyl groups.[62]

Because it is probable that hydrophobic hydration (solvation) packed Chl *a*/*a*′ molecules into a small space in the aqueous solution and resulted in the formation of the Chl aggregates, the structure of the aqueous solvent should be correlated to the Chl aggregation, which is consistent with our previous finding on the dependence of the Chl aggregation on the composition of aqueous methanol.[33] A study on the relationship between the Chl aggregation and the solvent structure can lead to an elucidation of the mechanisms of the aggregation and dissolution of Chl's in aqueous media. Further investigations are now underway.

**Acknowledgment.** We are grateful to Y. Imamura and M. Umetsu, Tohoku University, for their help in the SAXS experiments and to K. Hada, Shibaura Institute of Technology, for his help in the aggregation experiments.

## References and Notes

(1) Wagner, R. W.; Lindsey, J. S. *J. Am. Chem. Soc*. **1994**, *116*, 9759−9760.
(2) Jullien, L.; Canceil, J.; Valeur, B.; Bardez, E.; Lehn, J. M. *Angew. Chem., Int. Ed. Engl*. **1994**, *33*, 2438−2439.
(3) Osuka, A.; Maruyama, K.; Yamazaki, I.; Tamai, N. *Chem. Phys. Lett*. **1990**, *165*, 392−396.
(4) Yamazaki, I.; Tamai, N.; Yamazaki, T. *J. Phys. Chem*. **1990**, *94*, 516−525.
(5) Tamiaki, H.; Miyatake, T.; Tanikaga, R.; Holzwarth, A. R.; Schaffner, K. *Angew. Chem., Int. Ed. Engl*. **1996**, *35*, 772−774.
(6) Nozawa, T.; Ohtomo, K.; Suzuki, M.; Nakagawa, H.; Shikama, Y.; Konami, H.; Wang, Z.-Y. *Photosynth. Res*. **1994**, *41*, 211.
(7) Mastuura, K.; Hirota, M.; Shimada, K.; Mimuro, M. *Photochem. Photobiol*. **1993**, *57*, 92.
(8) Holzwarth, A. R.; Schaffner, K. *Photosynth. Res*. **1994**, *41*, 225−233.
(9) Blankenship, R. E.; Olson, J. M.; Miller, M. In *Anoxygenic photosynthetic bacteria*; Blankenship, R. E., Madigan, M. T., Bauer, C. E., Eds.; Kluwer Academic Publishing: Dordrecht, The Netherlands, 1995; Chapter 20, pp 399−435.
(10) Worcester, D. L.; Michalski, T. J.; Katz, J. J. *Proc. Natl. Acad. Sci. U.S.A*. **1986**, *83*, 3791−3795.
(11) Kratky, C.; Dunitz, J. D. *J. Mol. Biol*. **1977**, *113*, 431−442.
(12) Wang, Z.-Y.; Umetsu, M.; Yoza, K.; Kobayashi, M.; Imai, M.; Matsushita, Y.; Niimura, N.; Nozawa, T. *Biochim. Biophys. Acta* **1997**, *1320*, 73−82.
(13) Kratky, C.; Dunitz, J. D. *Acta Crystallogr*. **1975**, *B31*, 1586−1589.
(14) Kratky, C.; Dunitz, J. D. *Acta Crystallogr*. **1977**, *B33*, 545−547.
(15) Kratky, C.; Isenring, H. P.; Dunitz, J. D. *Acta Crystallogr*. **1977**, *B33*, 547−549.
(16) Chow, H.; Serlin, R.; Strouse, C. E. *J. Am. Chem. Soc*. **1975**, *97*, 7230−7237.
(17) Watanabe, T.; Mazaki, H.; Nakazato, M. *Biochim. Biophys. Acta* **1987**, *892*, 197−206.
(18) Hynninen, P. H.; Sievers, G. *Z. Naturforsch*. **1981**, *36b*, 1000−1009.
(19) Watanabe, T.; Hongu, A.; Honda, K.; Nakazato, M.; Konno, M.; Saitoh, S. *Anal. Chem*. **1984**, *56*, 251−256.
(20) Lötjönen, S.; Hynninen, P. H. *Org. Magn. Reson*. **1981**, *16*, 304−308.
(21) Hynninen, P. H.; Lötjönen, S. *Magn. Reson. Chem*. **1985**, *23*, 605−615.
(22) Mazaki, H.; Watanabe, T. *Bull. Chem. Soc. Jpn*. **1988**, *61*, 2969−2970.
(23) Hynninen, P. H.; Wasielewski, M. R.; Katz, J. J. *Acta Chem. Scand*. **1979**, *B33*, 637−648.
(24) Hynninen, P. H. *J. Chromatogr*. **1979**, *175*, 89−103.
(25) Oba, T.; Kobayashi, M.; Yoshida, S.; Watanabe, T. *Anal. Sci*. **1996**, *12*, 281−284.
(26) Hynninen, P. H. *Z. Naturforsch*. **1984**, *39b*, 675−678.
(27) Hynninen, P. H.; Lötjönen, S. *Synthesis* **1983**, 705−708.
(28) Shipman, L. L.; Cotton, T. M.; Norris, J. R.; Katz, J. J. *J. Am. Chem. Soc*. **1976**, *98*, 8222−8230.
(29) Sauer, K.; Lindsay-Smith, J. R.; Schultz, A. J. *J. Am. Chem. Soc*. **1966**, *88*, 2681−2688.
(30) Leicknam, J.-P.; Henry, M.; Kleo, J. *J. Chem. Phys*. **1978**, *75*, 529−534.
(31) Watanabe, T.; Kobayashi, M.; Hongu, A.; Oba, T. *Chem. Lett*. **1992**, *1847−1850*.
(32) Oba, T.; Watanabe, T.; Mimuro, M.; Kobayashi, M.; Yoshida, S. *Photochem. Photobiol*. **1996**, *63*, 639−648.
(33) Oba, T.; Mimuro, M.; Wang, Z.-Y.; Nozawa, T.; Yoshida, S.; Watanabe, T. *J. Phys. Chem. B* **1997**, *101*, 3261−3268.
(34) Maeda, H.; Watanabe, T.; Kobayashi, M.; Ikegami, I. *Biochim. Biophys. Acta* **1992**, *1099*, 74−80.
(35) Maeda, H.; Sonoike, K.; Watanabe, T. *J. Photochem. Photobiol., B* **1983**, *20*, 139−143.
(36) Sherman, G.; Wang, S. *Nature* **1966**, *212*, 588−590.
(37) Sherman, G.; Linchitz, H. *Nature* **1967**, *215*, 511.
(38) Jacobs, E. E.; Holt, A. S.; Kromhout, R.; Rabinowitch, E. *Arch. Biochem. Biophys*. **1957**, *72*, 495−511.
(39) Ballschmiter, K.; Katz, J. J. *Nature* **1968**, *220*, 1231−1233.
(40) Katz, J. J.; Ballschmiter, K.; Garcia-Morin, M.; Strain, H. H.; Uphaus, R. A. *Proc. Natl. Acad. Sci. U.S.A*. **1968**, *60*, 100−107.
(41) Ballschmiter, K.; Katz, J. J. *J. Am. Chem. Soc*. **1969**, *91*, 2661−2677.
(42) Ballschmiter, K.; Katz, J. J. *Biochim. Biophys. Acta* **1972**, *256*, 307−327.
(43) Koyama, Y.; Umemoto, Y.; Akamatsu, A.; Uehara, K.; Tanaka, M. *J. Mol. Struct*. **1986**, *146*, 273−287.
(44) Boldt, N. J.; Donohoe, R. J.; Birge, R. R.; Bocian, D. F. *J. Am. Chem. Soc*. **1987**, *109*, 2284−2298.
(45) Fujiwara, M.; Tasumi, M. *J. Phys. Chem*. **1986**, *90*, 250−253.
(46) Krawczyk, S. *Biochim. Biophys. Acta* **1989**, *976*, 140−149.
(47) Sidolov, A. N.; Terenin, A. N. *Opt. Spektrosk*. **1960**, *8*, 254−259.
(48) Ballschmiter, K.; Truesdell, K.; Katz, J. J. *Biochim. Biophys. Acta* **1969**, *184*, 604−613.
(49) Ballschmiter, K.; Cotton, T. M.; Strain, H. H.; Katz, J. J. *Biochim. Biophys. Acta* **1969**, 180, 347−359.
(50) Cotton, T. M.; Loach, P. A.; Katz, J. J.; Ballschmiter, K. *Photochem. Photobiol*. **1978**, *27*, 735−749.
(51) Hynninen, P. H.; Lötjönen, S. *Biochim. Biophys. Acta* **1993**, *1183*, 381−387.
(52) Thibodeau, D. L.; Koningstein, J. A. *J. Phys. Chem*. **1989**, *93*, 7713−7717.
(53) Kooyman, R. P. H.; Schaafsma, T. J. *J. Am. Chem. Soc*. **1984**, *106*, 551−557.
(54) Uehara, K.; Hioki, Y.; Mimuro, M. *Photochem. Photobiol*. **1993**, *58*, 127−132.
(55) Hochstrasser, R. M.; Kasha, M. *Photochem. Photobiol*. **1964**, 3, 317−331.
(56) Israelachvili, J. N.; Mitchell, D. J.; Ninham, B. W. *J. Chem. Soc., Faraday Trans. 1* **1976**, *72*, 1525−1568.
(57) As a reviewer pointed out, the possibility of a "weakened" Mg‥·OH‥O═C interaction in the Chl *a*′ aggregate cannot be fully excluded. This interaction is as weak as the Mg‥O═C interaction as judged from the wavenumber positions of the C13[1]-keto band and could give only a slight (less than 1 $cm^{-1}$)[58] spectral change on the deuteration of the solvents. The barely detectable deuteration effect and the weak intermolecular linkage like the Mg‥O═C interaction could be attributed to the postulated weakened Mg‥OH‥O═C interaction, but we think that it is natural to interpret that there is *practically* no Mg‥OH‥O═C interaction because the formation of the Chl aggregates in the aqueous media does not necessarily require hydrogen bondings between the Chl molecules. In the packed structure of the Chl *a*′ aggregate colloid, hydrophobic interaction[59] and van der Waals interaction, especially between the C17-long chains, may mainly stabilize the whole aggregate particle, though the hydrogen bonding can maintain the local structure of the macrocycle array. This should be distinguished from the role of water (or alcohol) molecules in the folding of the covalently linked Chl dimers in nonpolar solvents: hydrogen bonding must at any cost draw a macrocycle aside the other one. Our view is also supported by the finding that the carbonyl stretching region of the IR spectrum of the Chl *a*′ aggregate precipitate did not change upon exposure to water vapor.
(58) Hildebrandt, P.; Tamiaki, H.; Holzwarth, A. R.; Schaffner, K. *J. Phys. Chem*. **1994**, *98*, 2192−2197.
(59) Israelachvili, J.; Pashley, R. *Nature* **1982**, *300*, 341−342.
(60) Hunter, C. A.; Sanders, J. K. M. *J. Am. Chem. Soc*. **1990**, *112*, 5525−5534.
(61) Katz, J. J.; Shipman, L. L.; Cotton, T. M.; Janson, T. J. In *Porphyrins*; Dolphin, D., Ed.; Academic Press: New York, 1978; Vol. 5, pp 401−458.
(62) Uedaira, H.; Ikura, M.; Uedaira, H. *Bull. Chem. Soc. Jpn*. **1989**, *62*, 1−4.